Melt Blending of Ethylene–Vinyl Alcohol Copolymer/Clay Nanocomposites: Effect of the Clay Type and Processing Conditions

N. ARTZI,[1] Y. NIR,[1] M. NARKIS,[1] A. SIEGMANN[2]

[1]Department of Chemical Engineering, Technion–Israel Institute of Technology, Haifa 32000, Israel

[2]Department of Materials Engineering, Technion–Israel Institute of Technology, Haifa 32000, Israel

Received 14 June 2001; revised 10 May 2002; accepted 23 May 2002

ABSTRACT: Ethylene–vinyl alcohol copolymer (EVOH)/clay nanocomposites were prepared via dynamic melt blending. The effect of the processing parameters on blends containing two clay types in different amounts was examined. The blends were characterized with a Brabender plastograph and capillary rheometer, differential scanning calorimetry, dynamic mechanical thermal analysis (DMTA), X-ray diffraction (XRD), transmission electron microscopy (TEM), and thermogravimetric analysis (TGA). XRD showed advanced EVOH intercalation within the galleries, whereas TEM images indicated exfoliation, thereby complementing the XRD data. A dilution process with EVOH and clay treatment in an ultrasonic bath before melt blending did not add to the intercalation level. Different trends were observed for the EVOHs containing two different clay treatments, one claimed to be treated for EVOH and the other for amine-cured epoxy. They reflected the differences in the amounts of the strongly interacting polymer for the two nanocomposites. Thermal analysis showed that the melting temperature, crystallization temperature, and heat of fusion of the EVOH matrix sharply decreased with both increasing clay content and processing times. Significantly higher viscosity levels were obtained for the blends in comparison with those of the neat polymer. The DMTA spectra showed higher glass-transition temperatures for the nanocomposites in comparison with those of the neat EVOH. However, at high clay loadings, the glass-transition temperature remained constant, presumably because of an adverse plasticizing effect of the low moleculared mass onium ions treating the clays. The storage modulus improved when clay treated for EVOH was used, and it deteriorated when amine-cured epoxy clay was incorporated, except for the sonicated clay. TGA results showed significant improvements in the blends' thermal stability in comparison with that of the neat EVOH, which, according to TEM, was greater for the intercalated structures rather than for exfoliated ones. J Polym Sci Part B: Polym Phys 40: 1741–1753, 2002

Keywords: nanocomposites; ethylene–vinyl alcohol (EVOH); clay; intercalation; exfoliation; melt

INTRODUCTION

Composites consisting of nanoparticles dispersed in a polymer matrix may exhibit remarkable property enhancements with respect to conventional particulate composites. Layered silicates dispersed as a reinforcing phase in an engineering polymer matrix are among the most important forms of such nanocomposites. Conventional polymer/clay composites containing aggregated nanolayer tactoids ordinarily exhibit improved rigidity but often also show reduced strength, elon-

Correspondence to: M. Narkis (E-mail: narkis@tx.technion.ac.il)

Journal of Polymer Science: Part B: Polymer Physics, Vol. 40, 1741–1753 (2002)

gation, and toughness.[1] However, nanocomposites exhibit improved moduli without sacrificing strength and ductility, decreased thermal expansion coefficients, decreased gas permeability, and increased swelling resistance. The transition from conventional composites to nanocomposites requires the clay particles to undergo polymer intercalation and, subsequently, platelet exfoliation. Polymer melt intercalation is a promising approach for fabricating polymer/layered-silicate nanocomposites with conventional polymer processing techniques.[2] Intercalation may be formed by the static heating of a mixture of a polymer and a layered silicate above the melting temperature (T_m) of the polymer. This process can be facilitated with dynamic processes, such as compounding and melt processing.[3] A previous study suggested that under such dynamic conditions, in addition to clay particle fracturing, an onionlike delamination process may occur.[4] When the external clay layers are subjected to dynamic high shear stresses, single platelets may delaminate from the layered particles forming the original clay aggregates. This study focuses on the effect of different organically treated clays and processing conditions on the intercalation and exfoliation levels and on the resulting thermal and dynamic mechanical behavior of the generated nanocomposites.

EXPERIMENTAL

Materials

The ethylene–vinyl alcohol copolymer (EVOH) used in this study was a commercial product, containing 32 mol % ethylene, of Kuraray (Japan). Two types of treated clay were used. Nanomer-I.30E (E-clay) was an onium ion-modified montmorillonite mineral. Degradation began at temperatures higher than 300 °C. The organoclay contained 70–75 wt % montmorillonite and 25–30 wt % octadecylamine. It was claimed to be designed for ease of dispersion into amine-cured epoxy resins to form nanocomposites. Nanomer-I.35L (L-clay), a modified montmorillonite mineral containing 60–70 wt % montmorillonite and 30–40 wt % poly(oxyethylene decyloxypropylamine), was claimed to be treated for EVOH resins. Both were obtained from Nanocor (Illinois). The thermal stability of the clays, studied at the melt processing temperature, was confirmed by thermogravimetric analysis (TGA) tests.

Preparation Methods

Before melt blending, EVOH was ground into a powder. The polymer and clay powders were dried *in vacuo* at 80 and 60 °C, respectively, for 15 h. The components were dry-blended at selected ratios and subsequently melt-mixed in a Brabender plastograph equipped with a 50-cm^3 cell at 230 °C and 60 rpm for different periods of times (10–45 min). All the resulting blends were compression-molded at 230 °C and 980 MPa into 3-mm-thick plaques and were subsequently characterized. Some of the E-clay was treated for 24 h in a deionized water ultrasonic bath. The clay was then vacuum-filtered and dried at 70 °C for 24 h. The purpose of the ultrasonic bath before melt blending was to reduce interlayer interactions and thereby ease the subsequent intercalation and exfoliation steps.

Characterization

Differential scanning calorimetry (DSC) was employed to characterize the thermal behavior of the composites. A Mettler DSC 30 system, under a nitrogen atmosphere, at a heating rate of 10 °C/min was used. Samples were heated to a temperature above their T_m, cooled at the same rate, and subsequently reheated. The melting behavior was determined from the second heating run. The reduced enthalpy was normalized to the EVOH content. Dynamic mechanical properties of the compression-molded samples were measured with a dynamic mechanical thermal analysis (DMTA) system (PerkinElmer series 7) in the three-point bending mode. The system was operated at 1 Hz, under a nitrogen atmosphere, at a heating rate of 3 °C/min. The structure of the composites was examined with a Philips X'PERT X-ray diffraction (XRD) system with a Cu Kα radiation source operated at 40 kV and 40 mA and at a scanning rate of 0.5°/min. The blends' phase morphology was studied by electron microscopy. A JEOL JSM 5400 scanning electron microscope was employed for the observation of freeze-fractured and microtomed surfaces. All samples were gold-sputtered before observation. A Philips CM120 transmission electron microscope operated at 120 kV was also used. The images were taken at a nominal underfocus of 4–7 nm, where any amplitude contrast was enhanced with phase contrast. Im-

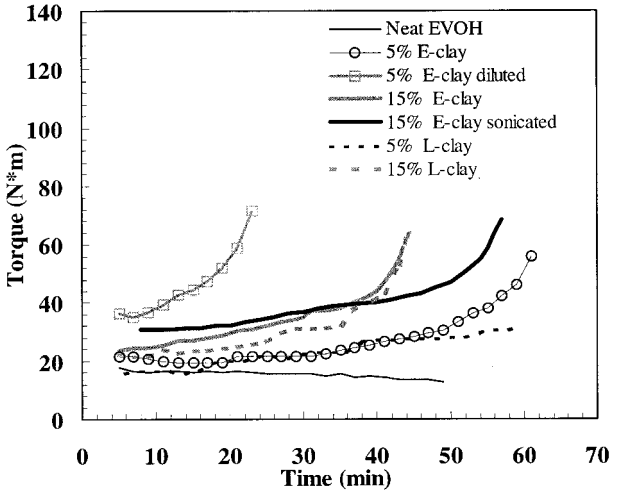

Figure 1. Brabender plastograms of neat EVOH, 85/15 EVOH/E-clay, 85/15 EVOH/sonicated E-clay, 95/5 EVOH/E-clay, 95/5 EVOH/E-clay diluted from 85/15 EVOH/E-clay with fresh EVOH, 85/15 EVOH/L-clay, and 95/5 EVOH/L-clay at 230 °C and 60 rpm.

ages were recorded digitally with a Gatan 791 MultiScan charge coupled device (CCD) camera and the Digital Micrograph 3.1 software package. Ultrathin sections were prepared at room temperature with a Reichert Ultracut E ultramicrotome with a glass knife. The apparent viscosity of the melt-mixed samples was measured at 230 °C with an MCR capillary rheometer mounted on an Instron TT-D. A capillary 5 cm (2 in.) in length and 0.127 cm (0.05 in.) in diameter (L/D = 40) was employed. The extrudate velocity exiting the rheometer die was controlled by the crosshead speed, ranging from 0.05 to 50 cm/min. The force required to maintain the desired volumetric rate was recorded. The samples were further characterized with a TA 2050 thermogravimetric analyzer. Samples were heated under an air atmosphere at a heating rate of 20 °C/min, with the sample weight loss monitored.

RESULTS AND DISCUSSION

Brabender Compounding

EVOH/clay mixtures were melt-blended in a Brabender plastograph cell.[4] Figure 1 shows the mixing torque as a function of the mixing time for the following systems: neat EVOH, 85/15 EVOH/E-clay, 85/15 EVOH/sonicated E-clay, 95/5 EVOH/E-clay, 95/5 EVOH/E-clay diluted from 85/15 EVOH/E-clay with fresh EVOH, 85/15 EVOH/L-clay, and 95/5 EVOH/L-clay. Two main observations can be made: the plastograms are affected by the clay content, and most of them show an abrupt torque upturn. The latter was suggested[4] to result from particle fragmentation, delamination, and the formation of particle networks. The time required for the torque to show a viscosity upturn decreases with the clay content. This trend is similar for the two types of clay studied. Interestingly, with the blending of the 85/15 EVOH/E-clay and fresh EVOH, it takes only 10 min for the torque to rise abruptly and form the 5 wt % EVOH/E-clay composite. It seems that a well-designed compounding/kneading machine should have the potential of producing EVOH/clay nanocomposites in a single-compounding-step operation. In another experiment meant to weaken the interlayer forces, the clay was treated in an ultrasonic bath before melt blending. Initially, the torque for the 85/15 EVOH/sonicated E-clay is higher than that of the EVOH/E-clay containing the as received E-clay; however, the abrupt torque rise occurs after a longer time for the former (sonicated). This behavior indicates that the original clay aggregates were ultrasonically fractured at weak planes into smaller aggregates, which resulted in the initial higher melt viscosity. However, the longer mixing time required may indicate that peeling off platelets from the smaller fragmented clay particles is more difficult than from the larger original aggregates. In polymer solution blending with clay or the blending of a polymerizing monomer with clay, intercalation precedes exfoliation, whereas in dynamic melt blending of the EVOH/clay systems, both intercalation and exfoliation processes simultaneously take place along with direct delamination, as we showed previously.[4] This is in agreement with Dennis et al.,[5] who found that clay fracturing is a result of shearing stacks of platelets apart to make the stacks thinner. Moreover, platelets subjected to dynamic high shear forces are delaminated by peeling apart. Although ultrasonic treatment is known to be useful for solution and monomer intercalation, it may have an adverse effect on melt intercalation and delamination.

XRD

The gallery spacing between clay platelets within an aggregate structure is indicative of their extent of intercalation and can be determined with XRD.[6] Figure 2 shows the XRD pattern of neat

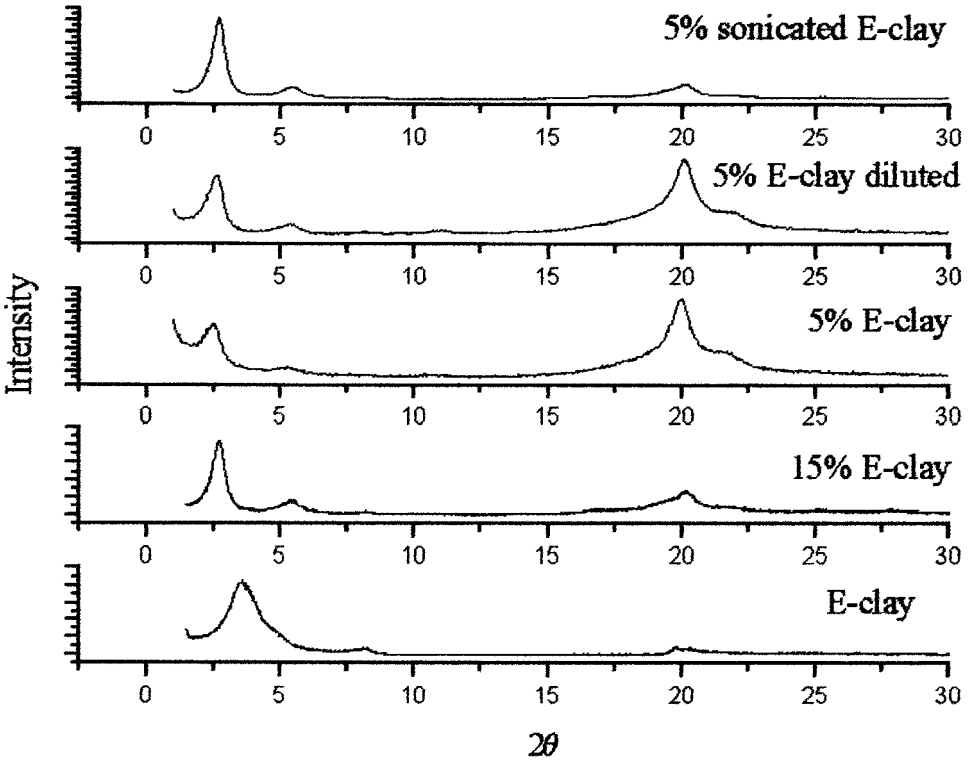

Figure 2. XRD patterns of neat EVOH, 85/15 EVOH/E-clay, as received and sonicated clay, and 95/5 EVOH/E-clay directly blended and diluted from 85/15 EVOH/E-clay prepared by 45 min of mixing in the Brabender cell at 230 °C.

E-clay, 85/15 EVOH/E-clay, 85/15 EVOH/sonicated E-clay, 95/5 EVOH/E-clay, and 95/5 EVOH/E-clay diluted from 85/15 EVOH/E-clay. All blends were characterized after melt mixing in the Brabender machine (as shown in Fig. 1) and compression molding. The increase in the basal spacing of the clay is higher for the lower clay contents. The neat E-clay shows a characteristic peak at $2\theta = 3.58°$ ($d_{001} = 25$ Å). The incorporation of 15 wt % E-clay into EVOH has resulted in an intercalated structure with a gallery spacing of 32 Å ($2\theta = 2.72$ °). The peaks seen in the small-angle range indicate an order within the composite.[7] The system containing 5 wt % clay exhibits a characteristic peak at 2.47° ($d_{001} = 36$ Å), and the diluted system containing 5 wt % clay shows a characteristic peak at 2.67° ($d_{001} = 33$ Å), similar to that of the 15 wt % E-clay system. It is suggested that the neat EVOH added at a second stage to form the diluted system has a small interaction level with the clay and acts mainly as a diluent. The peaks of the system containing 5% E-clay are broader than those of the corresponding diluted system and the 85/15 EVOH/E-clay. The highly ordered structure is also maintained in the diluted system, as indicated by the higher order X-ray reflection (Fig. 2). The characteristic peak of the sonicated E-clay is at 2.7° ($d_{001} = 33$ Å), very similar to that of the system containing 15 wt % original E-clay. The compounding of the L-clay results in a slight increase in the basal spacing (Fig. 3). The neat clay characteristic peak is at 3° ($d_{001} = 29$ Å), whereas the 15, 5, and 3 wt % composites show peaks at 2.7–2.8° ($d_{001} = 32$ Å). As the clay content decreases, the EVOH crystallinity is higher. The effect of processing time on the 97/3 EVOH/L-clay system was also studied. The characteristic peaks of these composites are approximately at 2.7° for 10–45 min; no clear difference is observed for the basal spacing.

Scanning Electron Microscopy (SEM)

Observation of the clay dispersion level within the polymer matrix by SEM was first performed on cryogenically fractured surfaces. EVOH/clay fractured surfaces (not shown here) are difficult to study because of the developed structure observed for the neat EVOH. Furthermore, as a result of the high EVOH/clay interaction levels, it

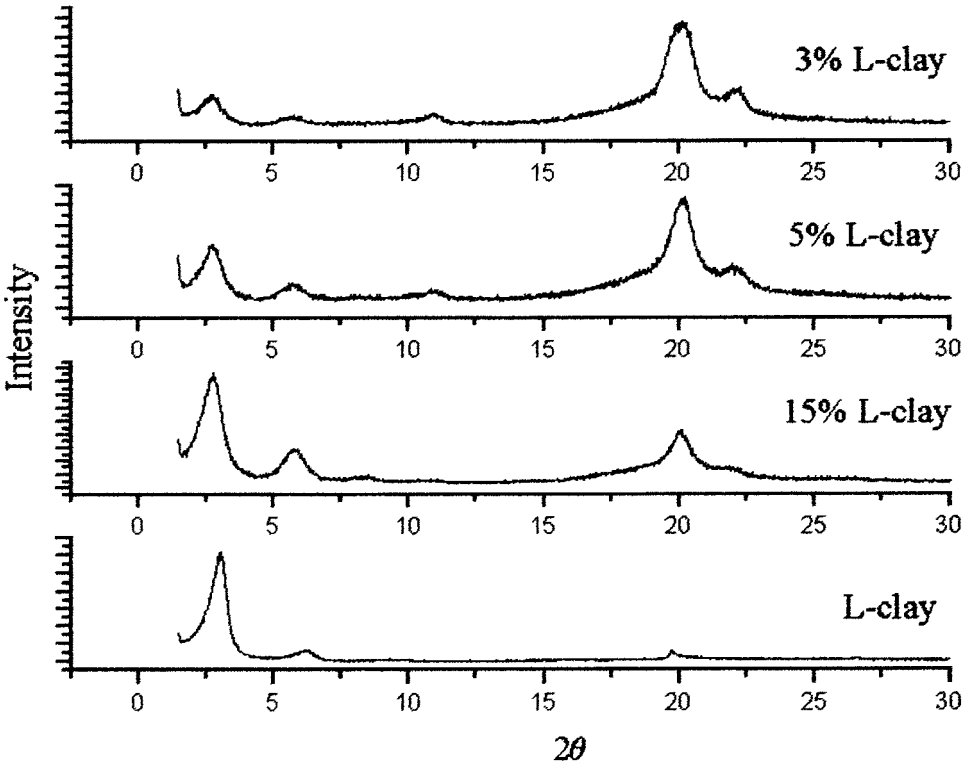

Figure 3. XRD patterns of neat EVOH and 97/3, 95/5, and 85/15 EVOH/L-clay prepared by 45 min of mixing in the Brabender cell at 230 °C.

is difficult to distinguish between the two phases. However, microtomed surfaces provide more coherent pictures. The morphology of 85/15 EVOH/E-clay, 85/15 EVOH/sonicated E-clay, 95/5 EVOH/E-clay, 95/5 EVOH/E-clay diluted from 85/15 EVOH/E-clay with fresh EVOH, 85/15 EVOH/L-clay, and 95/5 EVOH/L-clay is presented in Figure 4. Microtomed samples of neat EVOH (not shown here) exhibit a smooth surface area; therefore, observed foreign particles can be considered to represent the clay phase. The observed elongated voids represent clay particles pulled out by microtoming. Relatively low-magnification micrographs were used to monitor the dispersion of the clay particles within the polymer matrix and the average size of the clay aggregates. The microtomed surfaces show smaller clay particles for L-clay than for E-clay at 5 and 15 wt % clay contents [cf. Fig. 4(a,c) and Fig. 4(b,d)]. Moreover, the L-clay-containing blend shows significantly fewer clay particles than in the presence of E-clay for the same clay content, implying that the former clay has much smaller clay particles that are below SEM resolution. This is due to enhanced fracturing of the micrometer-scale clay aggregates in the Brabender cell. The fracturing process may eventually lead to dispersed single platelets in the continuous matrix, that is, delamination, without a preceding intercalation step. A comparison of the 5 wt % E-clay blends directly mixed or otherwise diluted from the 15 wt % clay blend [cf. Fig. 4(d) and Fig. 4(e)] reveals that the diluted system has larger clay particles. Therefore, the added neat EVOH polymer serves as a diluent, making this process less efficient than the direct process with respect to clay fracturing and delamination. In general, the blends' micrographs contain bimodal populations, aggregates larger than 15 μm and many small clay particles that have been fractured during melt mixing, differently from the raw clay characterized by particle distribution between 10 and 25 μm and not by modality. Figure 4(f) depicts EVOH containing 15 wt % sonicated E-clay. The 15 wt % sonicated clay blend shows fewer aggregates than the unsonicated one [cf. Fig. 4(f) and Fig. 4(b)], yet the observed remainder particles (of the smaller population size) are larger. The clay was probably fractured in the initial sonication step, and so fewer clay aggregates larger than 15 μm can be observed. However, there have been minor clay fracturing and delamination processes

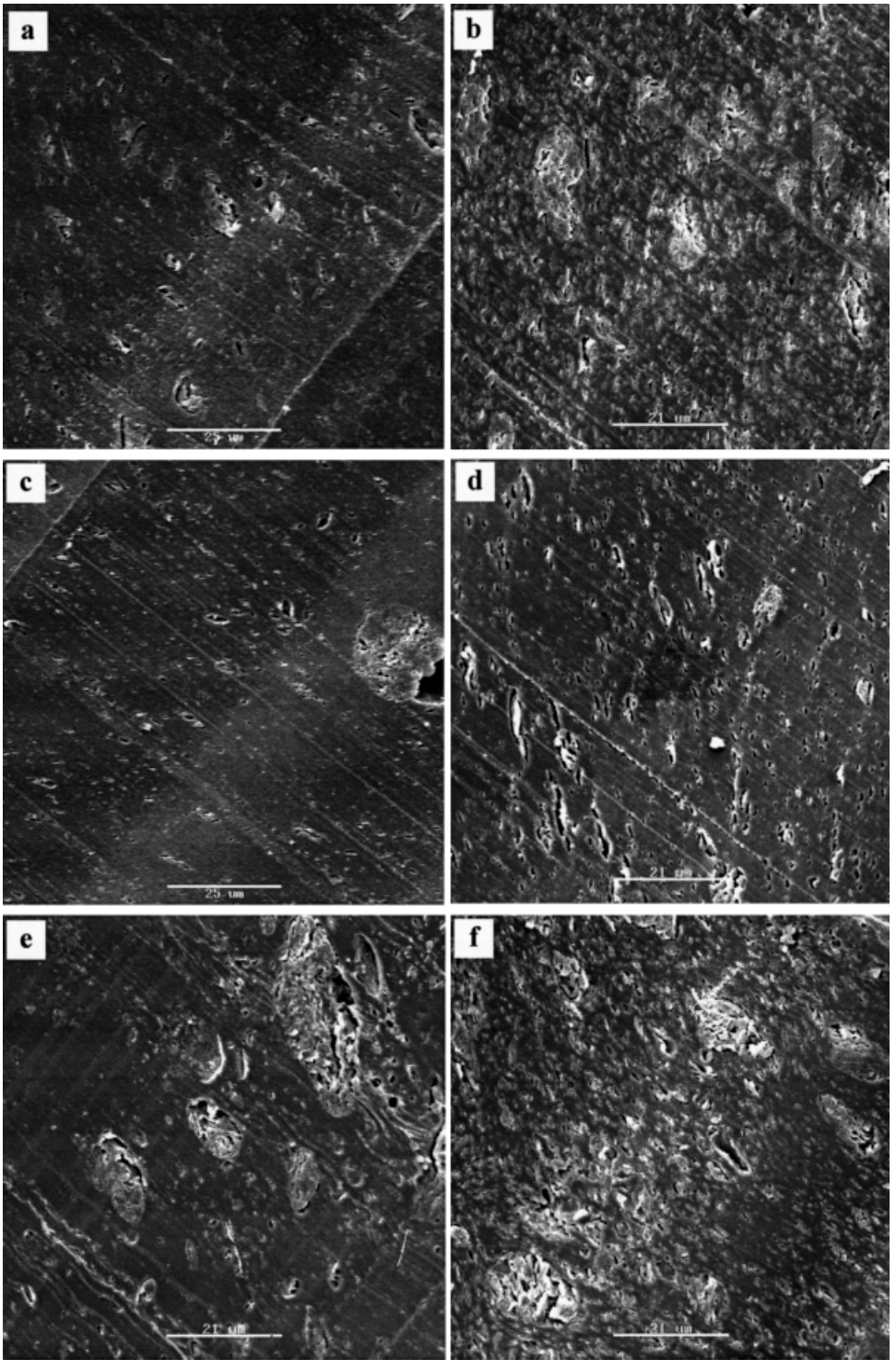

Figure 4. SEM micrographs of microtomed surfaces of EVOH/clay blends prepared by mixing in the Brabender cell, at 230 °C: (a) 85/15 EVOH/L-clay, (b) 85/15 EVOH/E-clay, (c) 95/5 EVOH/L-clay, (d) 95/5 EVOH/E-clay, (e) 95/5 EVOH/E-clay diluted from 85/15 EVOH/E-clay, and (f) 85/15 EVOH/sonicated E-clay.

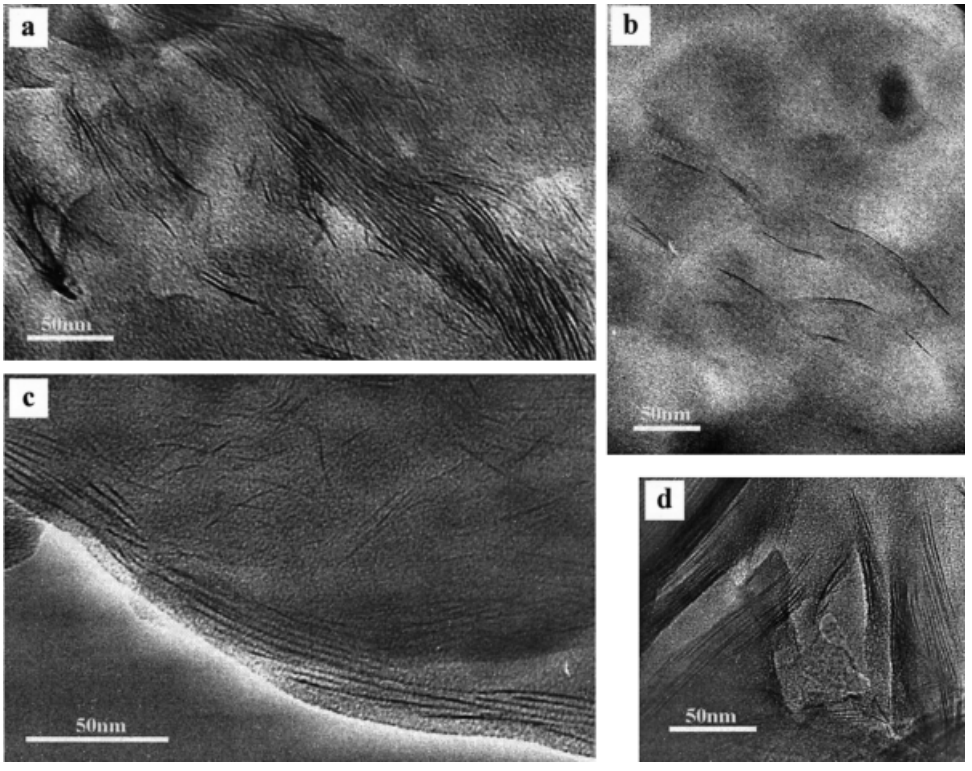

Figure 5. TEM micrographs of EVOH blends prepared by mixing in the Brabender cell at 230 °C (bar = 50 nm): (a) 95/5 EVOH/L-clay, (b) 95/5 EVOH/E-clay, (c) 85/15 EVOH/E-clay, and (d) 85/15 EVOH/L-clay.

during the melt blending of those smaller aggregates that ultimately lead to fewer small clay particles.

Transmission Electron Microscopy (TEM)

Individual silicate layers can be observed with TEM; therefore, TEM and XRD provide complementary data.[8] Figure 5 shows TEM images of EVOH containing 5 and 15 wt % clay of both types, E and L. The light gray area is the EVOH matrix, and the darker regions are made up of the silicate layers. Both intercalated and delaminated regions can be seen. The intercalated regions [Fig. 5(a,c,d)] have a microstructure similar to that of the treated clay (periodical ordered structure), but the interlayer distance is expanded to 3–4 nm, which is compatible with the XRD results. However, some of the silicate layers are exfoliated into nanometer layers and randomly dispersed in the polymer matrix via dynamic melt mixing [Fig. 5(a–c)]. The blends exhibit mixed morphology (intercalated and delaminated). The exfoliated structure is more evident at the lower clay content for both clay types [cf. Fig. 5(a,b) and Fig. 5(c,d)], as expected. However, the blend containing 5 wt % L-clay [Fig. 5(b)] shows regions of fully exfoliated structure.

Capillary Rheometer

The apparent viscosity of neat EVOH and EVOH containing 5 wt % clay for both clay types is presented in Figure 6. The rheology of various polymer layered-silicate nanocomposites was studied by Giannelis et al.[9] It was found that intercalated nanocomposites display a shear-thinning behavior at low shear rates, where the pure polymer displays a viscosity independent of the shear rate. In contrast, delaminated hybrids obey Newtonian-type behavior at low shear rates. The interpretation of EVOH/clay rheological behavior is complex because it contains anisotropic filler in both intercalated and delaminated states composed of tactoids of different sizes. Moreover, the neat EVOH displays shear-thinning behavior at low shear rates. However, the difference in the melt flow behavior relevant to the melt processing

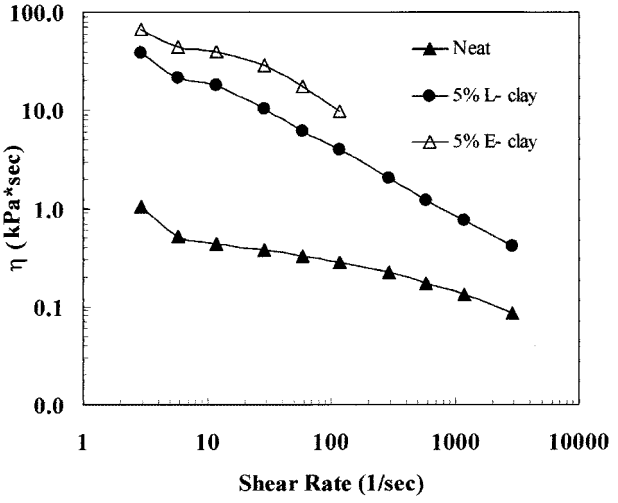

Figure 6. Apparent viscosity (η) versus the shear rate of neat EVOH, 85/15 EVOH/E-clay, 95/5 EVOH/E-clay, 85/15 EVOH/L-clay and 95/5 EVOH/L-clay at 230 °C.

of the blends containing different clay types may provide some insight into the size and distribution of the clay particles within the matrix. Both the composites and the neat polymer exhibit a typical pseudoplastic behavior. The apparent viscosity increases significantly when clay is incorporated, and the clay affects the viscosity throughout the entire range of shear rates studied. The studied range in the case of 5 wt % E-clay was limited by the too high force required, reaching the permitted force limit. Accordingly, higher clay contents could not be studied even at the lower levels of the shear rate. The viscosity increase is a result of the polymer/filler interaction and the formation of gel-like structures at the higher filler contents. The presently studied systems contain much lower clay contents than are usually used for micrometer-scale fillers; however, the effects on the melt rheology are significant, indicating the high interaction levels between EVOH and the treated clay, especially for the E-clay. These results are in agreement with the Brabender data showing an abrupt torque upturn after a certain mixing time that is shorter for E-clay than for L-clay. The increase in the viscosity even at the higher shear rates indicates the existence of platelets dispersed within the matrix. It is possible that these distributed platelets were produced during the melt blending by erosion of clay particles by the dispersive mixing process.[10] Because of their large exposed surface area, the apparent viscosity is affected, even at low clay contents.

DSC

The crystallization process in the presence of clay particles, especially clay platelets, was recently reported to result in smaller crystals, which cause lowering of both the melting temperature and enthalpy.[4] It is also suggested that in highly interacting systems (i.e., EVOH/treated clay), the high polymer/clay interaction level hinders the crystallization process, leading to smaller crystallites with defects and lower degrees of crystallization. This is in contrast to polyamide-6 nanocomposites, in which the high surface area of the silicate platelets and their chemical affinity for polyamide-6 have induced a nucleation and lamellar ordering effect.[11] DSC thermograms of neat EVOH, 85/15 EVOH/E-clay, 95/5 EVOH/E-clay, and 95/5 EVOH/E-clay diluted with fresh EVOH from 85/15 EVOH/E-clay are presented in Figure 7(a) showing second heating runs. Significant changes in the EVOH melting behavior are observed. Both T_m and the enthalpy of melting (ΔH_m) significantly decrease as the clay content increases; the T_m and ΔH_m reductions are 17.2 °C and 31.8 mJ/g and 20.1 °C and 35.5 mJ/g, for the 5 and 15 wt % clay composites, respectively, relative to the neat EVOH (179.6 °C and 82 mJ/g).

For the diluted system, the reduction in T_m and ΔH_m (13.7 °C and 28.9 mJ/g), in comparison with the neat EVOH, is smaller than that of the mixture directly blended at a ratio of 95/5 EVOH/E-clay. The EVOH added causes initially a torque/viscosity decrease when the system melts (compared to the system containing 15 wt % E-clay at the end of the mixing process) and subsequently an abrupt increase in the torque due to the platelet network of the already intercalated/exfoliated 85/15 EVOH/E-clay system. Therefore, the added EVOH acts essentially as a diluent, without causing further intercalation. The T_m value of the diluted system reflects a lower interaction level between the added, diluting EVOH and the clay surfaces. Figure 7(b) depicts crystallization runs of neat EVOH, 85/15 EVOH/E-clay, 95/5 EVOH/E-clay, and 95/5 EVOH/E-clay diluted with fresh EVOH from 85/15 EVOH/E-clay. The reduction in the crystallization temperature (T_c) is more pronounced as the clay content increases (22.4 and 26.6 °C for 5 and 15% clay, respectively), relative to the neat EVOH, because of the higher interruption of the crystallization process. However, the EVOH in the diluted system crystallizes at a higher temperature, 6.4 °C higher than that of the EVOH in the directly blended system. This

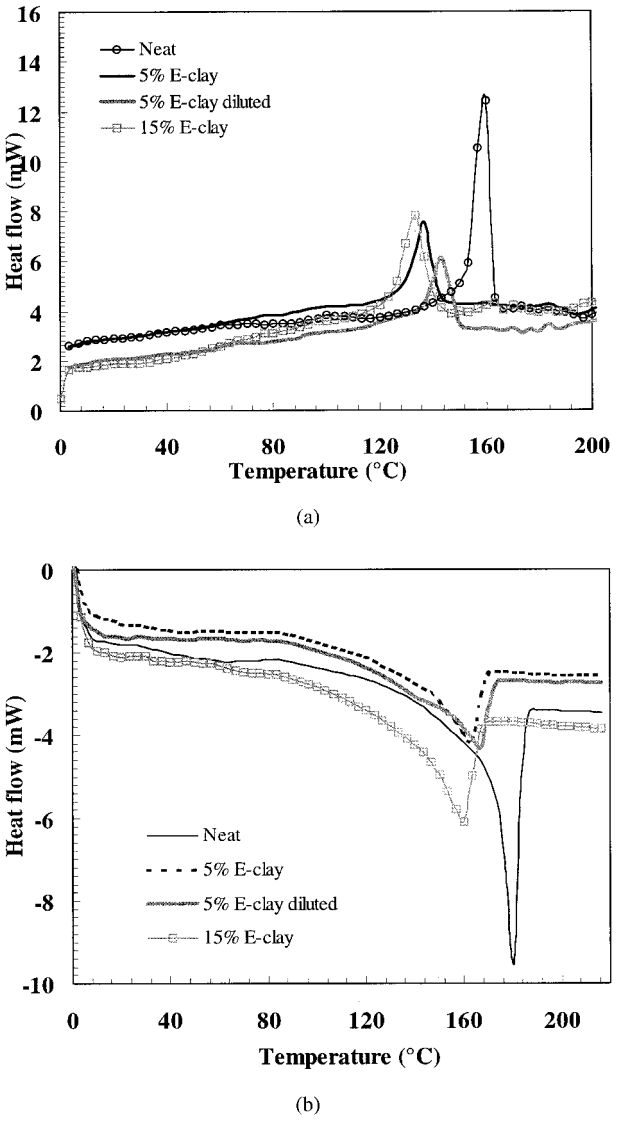

Figure 7. DSC (a) second heating runs and (b) cooling runs of neat EVOH, 85/15 EVOH/E-clay, and 95/5 EVOH/E-clay directly blended and diluted from 85/15 EVOH/E-clay prepared by 45 min of mixing in the Brabender cell at 230 °C.

behavior supports the suggestion that the EVOH added at the second stage does not significantly interact with the clay, leading to enhanced crystallization.

The effect of the sonicated treated clay on the thermal behavior is presented in Table 1. The reductions in T_m and enthalpy values of the EVOH, in the presence of the sonicated treated clay, are 14.4 °C and 25 mJ/g, respectively, in comparison with the neat EVOH. This reduction is lower than for the as-received treated clay blended with EVOH. Therefore, the thermal behavior of EVOH is less affected by the sonicated clay particles. The DSC results are, therefore, in agreement with the torque data shown in Figure 1.

Table 1 shows that the clay type plays an important role in determining the blend's thermal behavior. The reduction in T_m and enthalpy values is lower for EVOH in the presence of L-clay than in the presence of E-clay. The higher crystallization degree may be attributed to the lower degree of EVOH intercalation in the presence of L-clay. Because the intercalated polymer chains do not exhibit bulklike crystallization, the fraction of the crystalline polymer should represent the unintercalated fraction, as reported by Vaia et al.[3] As there is more bulk polymer in the presence of L-clay, less polymer is attached to the clay platelets, which may lead to the higher T_m in the presence of that clay. The reduction in T_m and enthalpy values in relation to the neat EVOH for the 5 wt % L-clay versus the 15 wt % L-clay (Table 1) is lower in comparison with the E-clay. T_c is higher in the presence of L-clay for both 5 and 15 wt % in comparison with the E-clay blends (Table 1). For the lower clay contents, a higher value of T_c was found for the two clay types that was due to less interruption of the crystallization process. A different processing duration for the 97/3 EVOH/L-clay has only a slight effect on T_m, enthalpy values, and T_c of the EVOH in the blend (Table 1). However, as processing time increases, the melting and crystallization peaks become broader (not shown here), showing higher crystallite size distribution.

DMTA

Organic onium ion low molecular reagents are frequently used for compatibilization, despite their function as undesirable plasticizers. The plasticizing effect may be clearly observed at high clay loadings.[12] The loss modulus curves [Fig. 8(a)] show a higher glass-transition temperature (T_g) value for EVOH containing 5 wt % E-clay than neat EVOH because of polymer/clay interactions. However, T_g decreases to its original value when the clay loading reaches 15 wt %, presumably because of the localized plasticizing effect of the low molecular weight onium ions. The diluted 5 wt % clay system has an intermediate T_g value between that of the neat polymer and the composite containing 5 wt % clay. This behavior supports the conclusion that the polymer part added at the second blending process fully participates in the flow process during melt blending but has a lower

Table 1. Thermal Characteristics of EVOH/Clay Nanocomposites

Material	T_c (°C)	ΔH_c (mJ/g)	T_m (°C)	ΔH_m (mJ/g)
Neat EVOH	159.7	60.4	179.6	82
EVOH + 15% E-clay	133.1	31.9	159.5	46.5
EVOH + 15% sonicated E-clay	143.1	43.2	165.2	56.7
EVOH + 5% E-clay	137.3	42.1	162.4	50.2
EVOH + 5% E-clay diluted	143.7	41.2	165.9	53.1
EVOH + 15% L-clay	140.7	31.8	164.1	54.3
EVOH + 5% L-clay	152.6	50.1	174.1	66.3
EVOH + 3% L-clay, 10 min	160.1	57.6	180.5	83.4
EVOH + 3% L-clay, 20 min	160.9	54.6	180.2	82
EVOH + 3% L-clay, 30 min	160.7	52.2	179.5	82.6
EVOH + 3% L-clay, 45 min	158.2	53.4	179.2	77.3

interaction level with the clay. As the clay content increases, damping is higher, representing a larger fraction of the amorphous phase, which supports the DSC results. Nevertheless, for the system containing 15 wt % sonicated clay, the damping is also higher, although the degree of crystallinity is higher, pointing out at another mechanism, such as internal friction.[13] Larger filler particles, namely those with lower surface area, are less effectively attached to the polymer chains, presumably leading to increased internal friction.[13] The EVOH/sonicated clay system has larger clay particles and shows a higher damping level. The storage modulus curves [Fig. 8(b)] show modulus reduction, in comparison with the neat EVOH, for all the studied composites throughout the entire temperature range (0–100 °C), except for the EVOH/sonicated clay composite. Although the filler particles are stiffer than EVOH, the plasticizing effect seems to be dominant, leading to the lower modulus values. The exceptional behavior of the EVOH/sonicated clay system is presently not clear. The modulus of the composites in the rubbery region (>50 °C) is lower than that of the neat polymer [Fig. 8(b)], presumably because of the reduction of the EVOH degree of crystallinity when clay is incorporated. This is also reflected by the lower DSC ΔH_m values. The clay type plays an important role for the mechanical properties. The loss modulus curves of EVOH/L-clay containing different amounts of clay (3, 5, and 15 wt %) are presented in Figure 9(a). Higher T_g values for the low clay contents are seen as a result of the high interaction level. This is compensated for the higher clay contents due to the plasticizing effect. Higher damping levels for the higher clay contents are attributed to the larger fraction of the amorphous phase. Interestingly, the storage modulus in the glassy state [Fig. 9(b)] is higher for all the studied composites in comparison with that of the neat polymer. This is in contrast to the behavior found in the presence of E-clay. The modulus increase, despite the previously described plasticizing effect, may stem from the presence of more delaminated platelets using L-clay, which compensates for the plasticization adverse effect. In the rubbery plateau region, only the modulus of the system containing 3 wt % clay remains higher than that of the neat EVOH because no crystallinity reduction occurs in that case. The effect of processing time is presented in Figure 10. The loss modulus curves of 97/3 EVOH/L-clay [Fig. 10(a)] show higher T_g values for the extended processing times (T_g's for the 30- and 45-min systems are similar). Because of the buildup of higher interaction levels, accompanied by fracturing and delamination processes generated during the longer mixing time, higher T_g values occur. This may also lead to restriction of mobility, as reflected by the higher temperatures for initiation of the damping peak. The storage modulus curves [Fig. 10(b)] show enhanced moduli for all the composites throughout the whole temperature range studied (there is no change in crystallinity). The storage modulus shows a significant maximum value for the 20-min-processed system. The modulus for 10-min processing is lower than that for 20 and 30 min, but it is similar to that for the 45-min processing. This may be a result of two different mechanisms: modulus enhancement with processing time resulting from the buildup of platelet networks and reduced modulus resulting from a degradation process of the polymer.

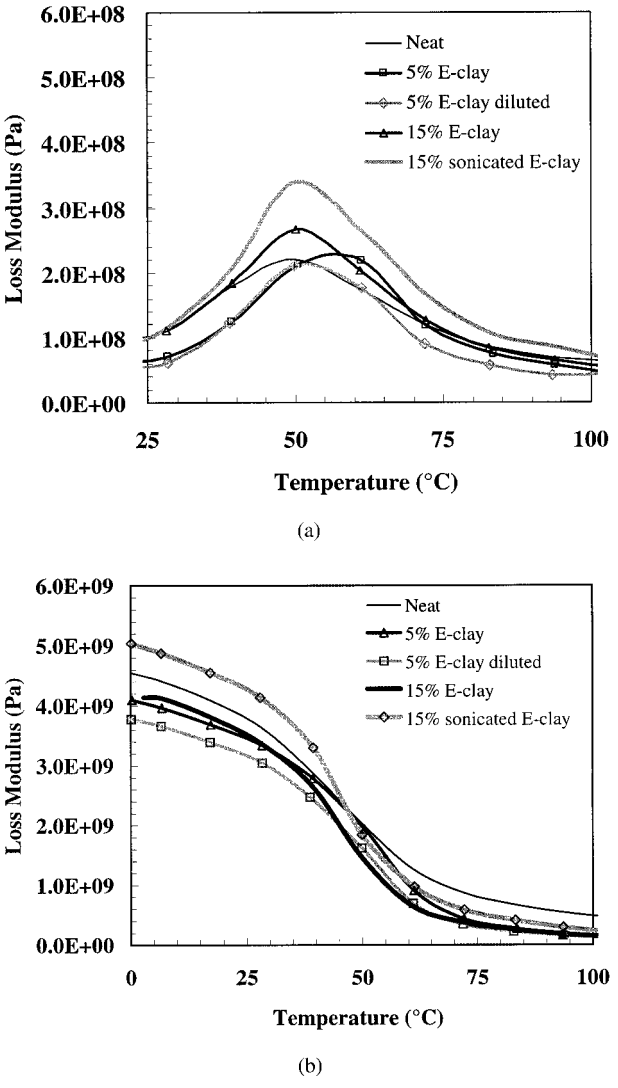

Figure 8. (a) Loss modulus and (b) storage modulus of neat EVOH, 85/15 EVOH/E-clay, 85/15 EVOH/sonicated E-clay, and 95/5 EVOH/E-clay directly blended and diluted from 85/15 EVOH/E-clay prepared by 45 min of mixing in the Brabender cell at 230 °C.

TGA

Figure 11 shows TGA thermograms of neat EVOH and EVOH containing 5 and 15 wt % E-clay and L-clay. The clay type and clay amount play an important role in the thermal stability of the blends. The decomposition temperature of neat EVOH is 403 °C (determined at a 50% mass loss). The decomposition temperature increases to 408 and 411 °C in the presence of 5 and 15 wt % L-clay and to 415 and 424 °C in the presence of 5 and 15 wt % E-clay, respectively. Therefore, the thermal stability is enhanced by the higher clay loadings. Furthermore, the thermal stability increases more significantly in the presence of E-clay than in the presence of L-clay for the two clay loadings. The clay platelets have a shielding effect on the matrix and slow the rate of mass loss of the decomposition products. The TGA results combined with the TEM observations actually show that the intercalated nanocomposite (containing E-clay) is more stable than the delaminated one (containing L-clay). This somewhat surprising result is in agreement with the other literature publications.[14,15]

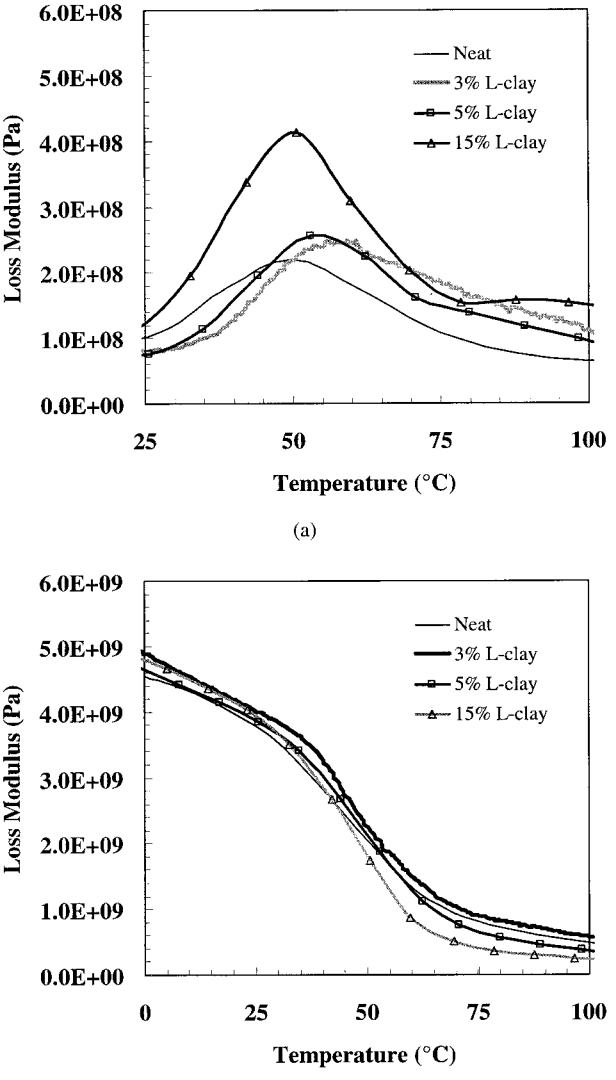

Figure 9. (a) Loss modulus and (b) storage modulus of neat EVOH and 97/3, 95/5, and 85/15 EVOH/L-clay prepared by 45 min of mixing in the Brabender cell at 230 °C.

CONCLUSIONS

Polymer/clay nanocomposites were produced with melt blending under dynamic conditions, where delamination and interlayer fracturing in addition to an intercalation process took place. XRD results showed that the gallery heights increased; larger changes were attained with the E-clay. TEM showed that the nanocomposites contained both intercalated and delaminated clay layers. The clay type played an important role in structuring during the melt-blending process. In the EVOH/clay system, both T_m and T_c of the polymer decreased with increasing clay content and processing time. The reduction was less significant when L-clay was used. Higher storage moduli were measured when L-clay was used. Opposite trends were observed for the E-clay composites; however, clay sonication before melt blending led to a higher modulus value in comparison with that of the neat EVOH. Higher melt viscosities were realized for the blends than for the neat polymer in capillary rheometry. This was attributed to the high EVOH/clay interaction level and the presence of fragmented smaller clay particles. The onium ions that treated the clays might act as undesirable plasticizers. The blends had higher thermal stability than the neat polymer, which according to TEM micrographs was more significant in the intercalated structures. In general, different treatments and processing conditions lead to property changes, which imply the significance of these parameters on the performance of the resulting nanocomposites.

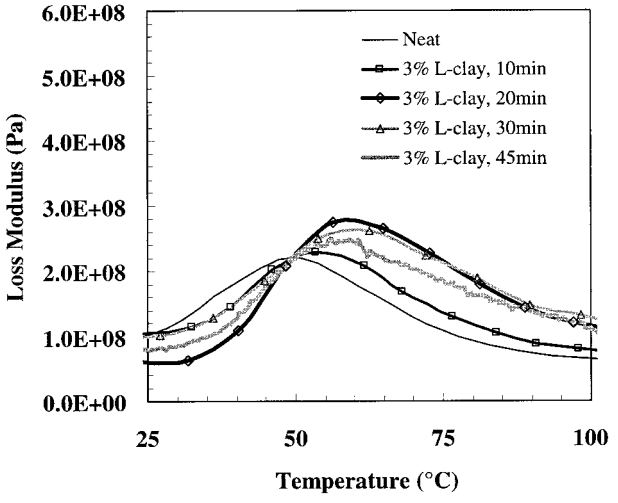

Figure 10. (a) Loss modulus and (b) storage modulus of neat EVOH and 97/3 EVOH/L-clay blends prepared at different processing times in the Brabender cell at 230 °C.

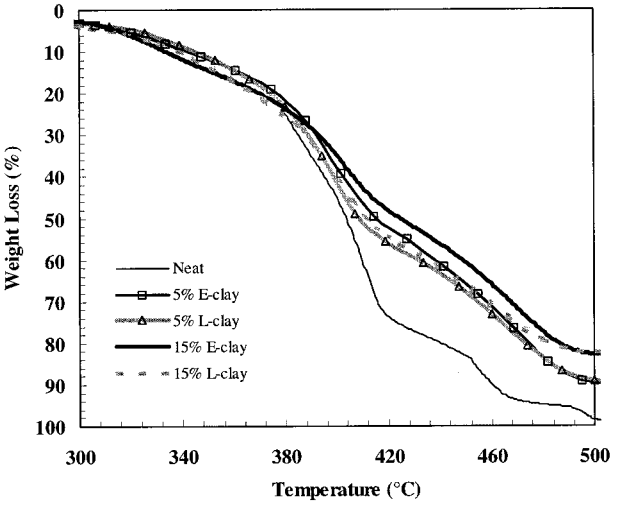

Figure 11. TGA analysis of neat EVOH, 85/15 EVOH/E-clay, 95/5 EVOH/E-clay, 85/15 EVOH/L-clay, and 95/5 EVOH/L-clay.

The authors are grateful to the Israel Ministry of Science and Culture for partially supporting the nanocomposite project. N. Artzi acknowledges the generous Levi Eshkol scholarship from the Israel Ministry of Science and Culture.

REFERENCES AND NOTES

1. LeBaron, P. C.; Wang, Z.; Pinnavaia, T. J. Appl Clay Sci 1993, 15, 11.

2. Giannnelis, E. P. Adv Mater 1996, 8, 29.
3. Vaia, R. A.; Jandt, K. J.; Kramer, E. J.; Giannelis, E. P. Chem Mater 1996, 8, 2628.
4. Artzi, N.; Nir, Y.; Wang, D.; Narkis, M.; Siegmann, A. Polym Compos 2001, 22, 710.
5. Dennis, H. R.; Hunter, D. L.; Cho, J. W.; Paul, D. R.; Chang, D.; Him, S.; White, J. L. Annu Tech Conf 2000, 2000, 428.
6. Lan, T.; Pinnavaia, T. J. Mater Res Soc Symp Proc 1996, 435, 79.
7. Vaia, R. A.; Jandt, K. D.; Kramer, E. J.; Giannelis, E. P. Macromolecules 1995, 28, 8080.
8. Zanetti, M.; Lomakin, S.; Camino, G. Macromol Mater Eng 2000, 279, 1.
9. Giannelis, E. P.; Krishnamoorti, R.; Manias, E. Adv Polym Sci 1999, 138, 107.
10. Zloczower, I. M.; Tadmor, Z. Mixing and Compounding of Polymers; Hanser: Munich, 1994.
11. Akkapeddi, M. K. Polym Compos 2000, 21, 576.
12. Wang, Z.; Pinnavaia, T. J. Book of Abstracts, American Chemical Society Proceedings, San Francisco, CA, March 26–30, 2000; American Chemical Society: Washington, DC, 2000.
13. Kalfoglou, N. K. J Appl Polym Sci 1986, 32, 5247.
14. Gilman, J. W. Appl Clay Sci 1999, 15, 31.
15. Gilman, J. W.; Jackson, C. L.; Moran, A. B.; Harris, R.; Manias, E.; Giannelis, E. P.; Wuthenow, M.; Hilton, D.; Phillips, S. Flame Retardants 2000, 49, 2000.